Kilonova as a probe of r-process nucleosynthesis

Gabriel Martínez-Pinedo

“The r-process and the nuclear EOS after LIGO-Virgo's third observing run”

INT Workshop, May 23-27, Seattle, USA

Helmholtz Forschungsakademie Hessen für FAIR

European Research Council
Established by the European Commission

ERC AdG KILONOVA

Collaborators

GSI theory

Ciências ULisboa

LIP

QUEEN'S UNIVERSITY BELFAST

ULB UNIVERSITÉ LIBRE DE BRUXELLES

UMONS Université de Mons

UNIVERSITÄT BIELEFELD

UAM Universidad Autónoma de Madrid

A. Bauswein, **A. Flörs**, O. Just, **G. Leck**, **L. Shingles**, N. Rahman, **V. Vijayan**, Z. Xiong
P. Amaro, J. P. Marques, J. M. Sampaio, **R. Silva**
S. Sim
J. Deprince, M. Godefroid, S. Goriely
H. Carvajal, P. Palmeri, P. Quinet
C. Robin
S. Giuliani, L. Robledo

R process modelling

Astrophysical environment should provide enough neutrons per seed for the r process to operate

$$A_{\mathrm{final}} = A_{\mathrm{initial}} + n_{\mathrm{seed}}$$

$\mathrm{n}_{\mathrm{seed}}$ depends mainly on neutron richness ejecta

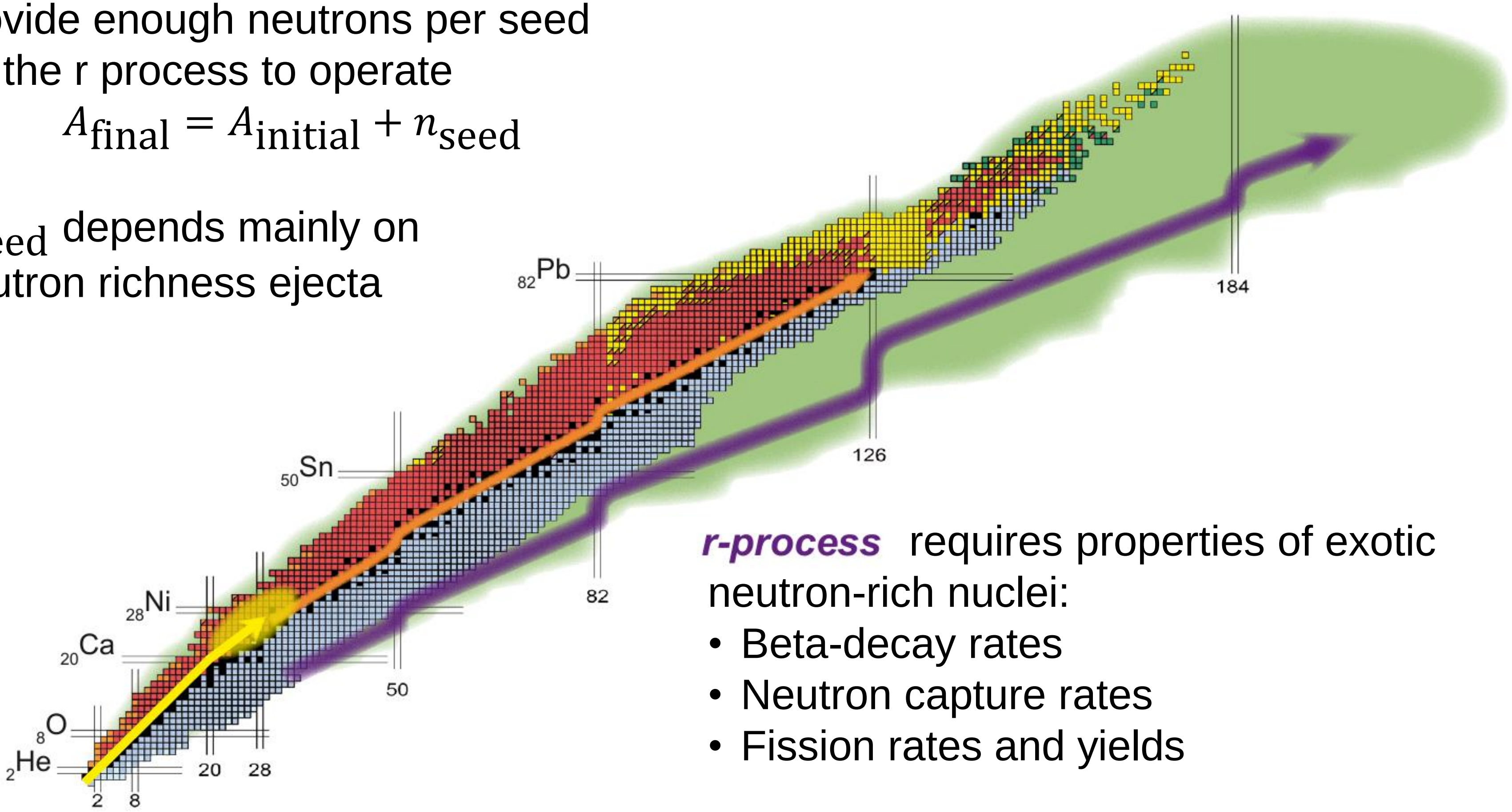

r-process requires properties of exotic neutron-rich nuclei:

- Beta-decay rates
- Neutron capture rates
- Fission rates and yields

Benchmark against observations:

- Indirect: Solar and stellar abundances (contribution many events, chemical evol.)
- Direct: Kilonova electromagnetic emission (single event, sensitive Atomic and Nuclear Physics)

Kilonova: signature of the r-process

Line of view GW170817

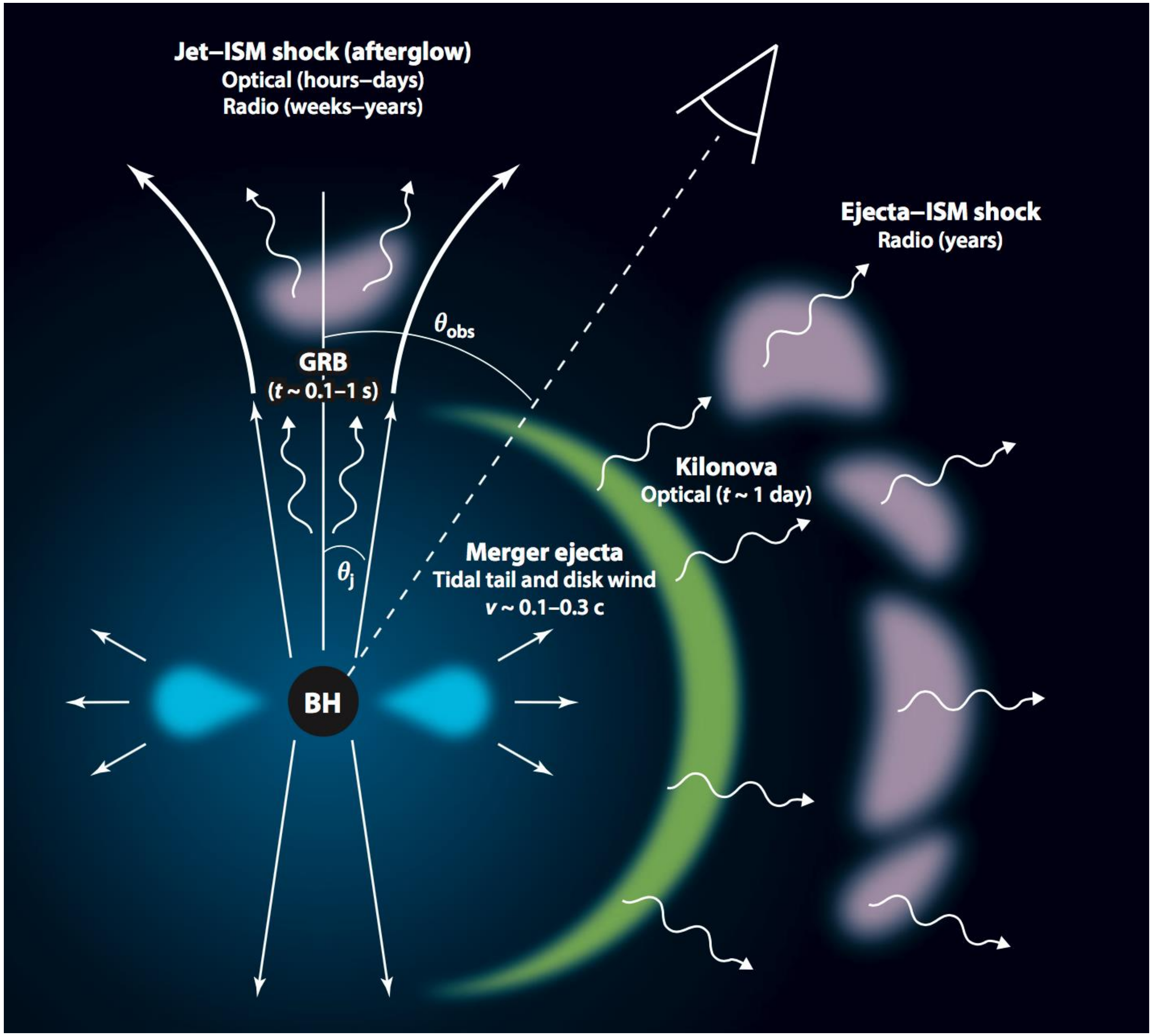

Metzger & Berger 2012

Kilonova: An electromagnetic transient due to long term radioactive decay of r-process nuclei

- Direct probe of the formation r-process nuclei
- Electromagnetic counterpart to Gravitational Waves
- Diagnostics physical processes at work during merger

R-process in mergers

Simulations

Bauswein et al, ApJ 773, 78 (2013)

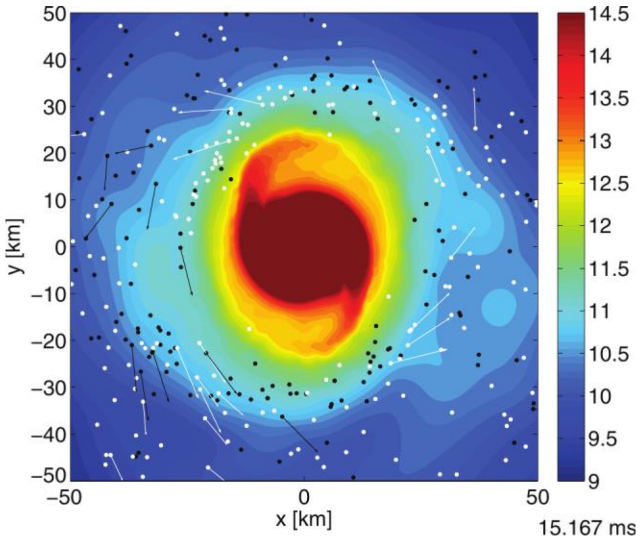

- Different sources of ejecta with different properties (Y_e)
- Role of equation of state
- Role of neutrinos

Nucleosynthesis

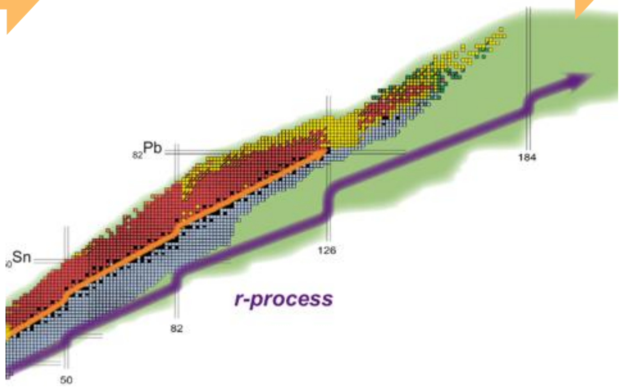

- Physics of neutron-rich and heavy nuclei

Light curve and spectra modelling

Watson et al, Nature **574**, 497 (2019)

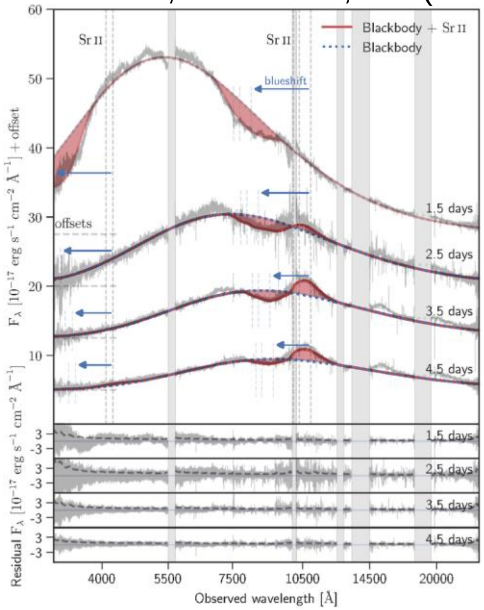

- Radioactive energy deposition
- Thermalization decay products (Barnes+ 2016, Kasen+ 2019)
- Spectra formation: atomic data depends on ejecta evolution (LTE vs NLTE)

Energy levels - Opacity

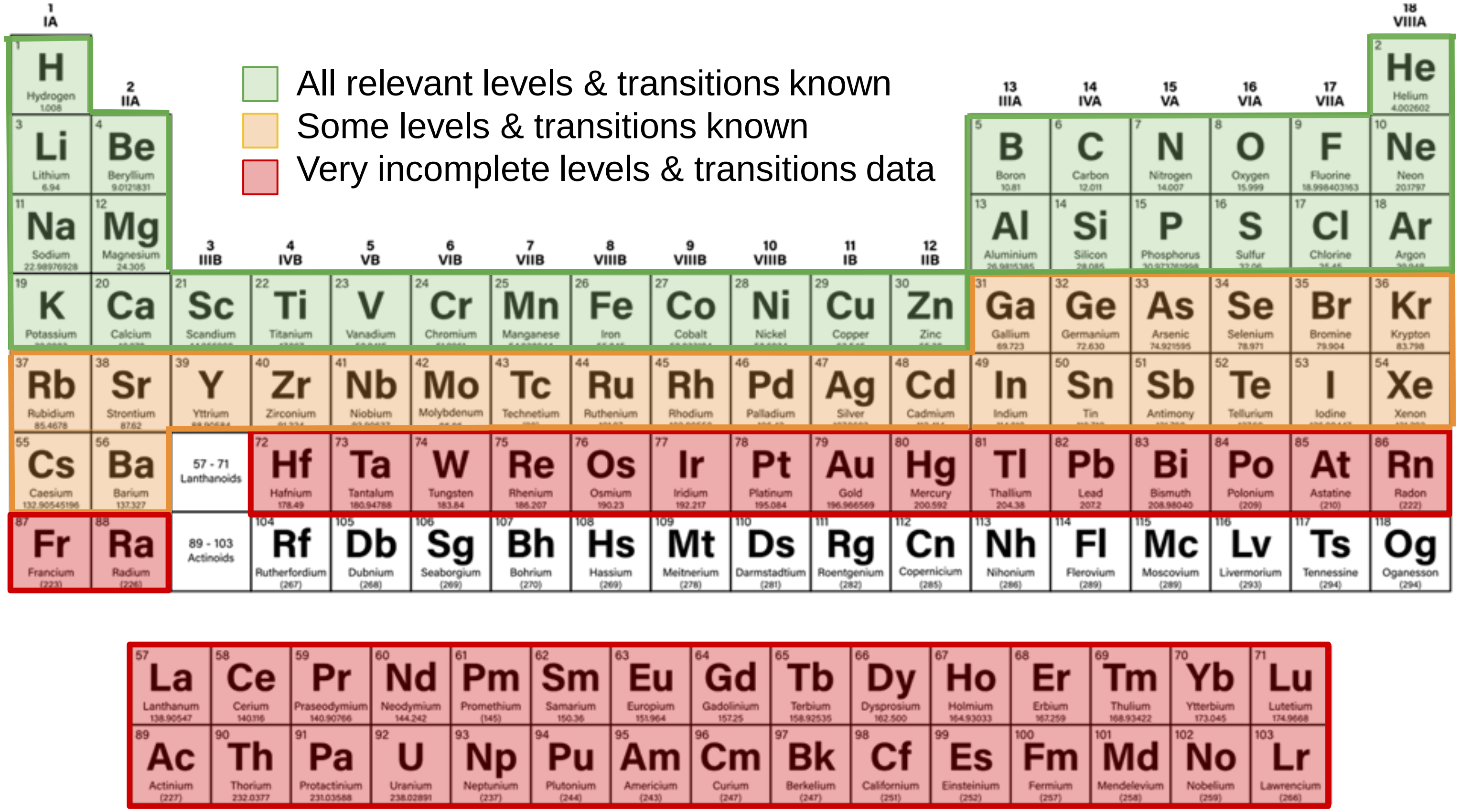

🟩 All relevant levels & transitions known
🟧 Some levels & transitions known
🟥 Very incomplete levels & transitions data

- Early evolution ($t \lesssim 1\,\mathrm{week}$, local thermodynamic equilibrium)
  - Bound-bound opacities
  - Not enough data: levels and transitions (theory: Gaigalas+ 2019, Tanaka+ 2020, Fontes+ 2020)
- Nebular evolution ($t \gtrsim 1\,\mathrm{week}$, non LTE)
  - Electron-ion cross sections, photoionization cross sections, recombination coefficients (Hotokezaka+ 2021, Pognan+ 2022)

Atomic opacities and spectral modelling

- Systematic opacity calculations
    - All elements between Iron and Actinides computed using Flexible Atomic Code [Gu CJP 86, 675 (2008), https://github.com/flexible-atomic-code/fac], U Lisbon same set of configurations than Tanaka et al 2020.
    - Extended set of configurations to ensure convergence low lying states and density of levels
    - Benchmark against data or calculations with alternative codes (HFR, U Mons)
- **TARDIS!**
  Kerzendorf & Sim, MNRAS 440, 387 (2014)
  https://tardis-sn.github.io/
    - 1D Monte Carlo Spectral Synthesis Code
    - Inner boundary: only early spectra possible

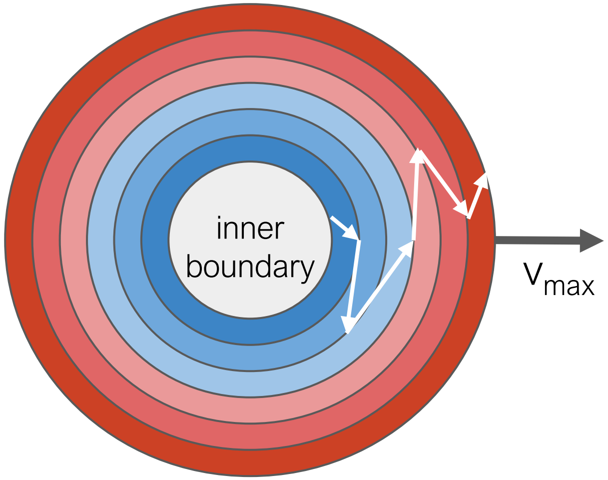

- **ARTIS** Kromer & Sim, MNRAS 398, 1809 (2009)
  https://github.com/artis-mcrt/artis
    - 3D Monte Carlo Radiative Transfer
    - Consistent description of energy deposition, transport and spectral formation
    - 3D geometry ejecta
    - Both photospheric and nebular epochs.

R. Silva

G. Leck

A. Flörs

L. Shingles

Atomic Opacities (LTE)

- Sobolev optical depth (for a line l)

Transition wavelength

$$\tau_l = \frac{\pi e^2}{m_e c} t \, f_l \; n_l \; \lambda_l$$

Oscillator strength

Population lower level
(Saha eq. and partition functions)

- Expansion opacity (homologous expanding material, not used in the radiation transport modelling)

$$\kappa_{\text{exp}}^{\text{bb}} = \frac{1}{\rho c t} \sum_l \frac{\lambda_l}{\Delta\lambda_{\text{bin}}} \left(1 - e^{-\tau_l}\right)$$

Ionization balance

- Lanthanides and Actinides: large contribution to opacity, more highly ionized than iron-group
  - Early phases: double ionized
  - After ~ 2 days: single ionized
- Single ionized material has higher bound-bound opacity than double ionized
- Ionization transition can potentially be observed in the spectrum

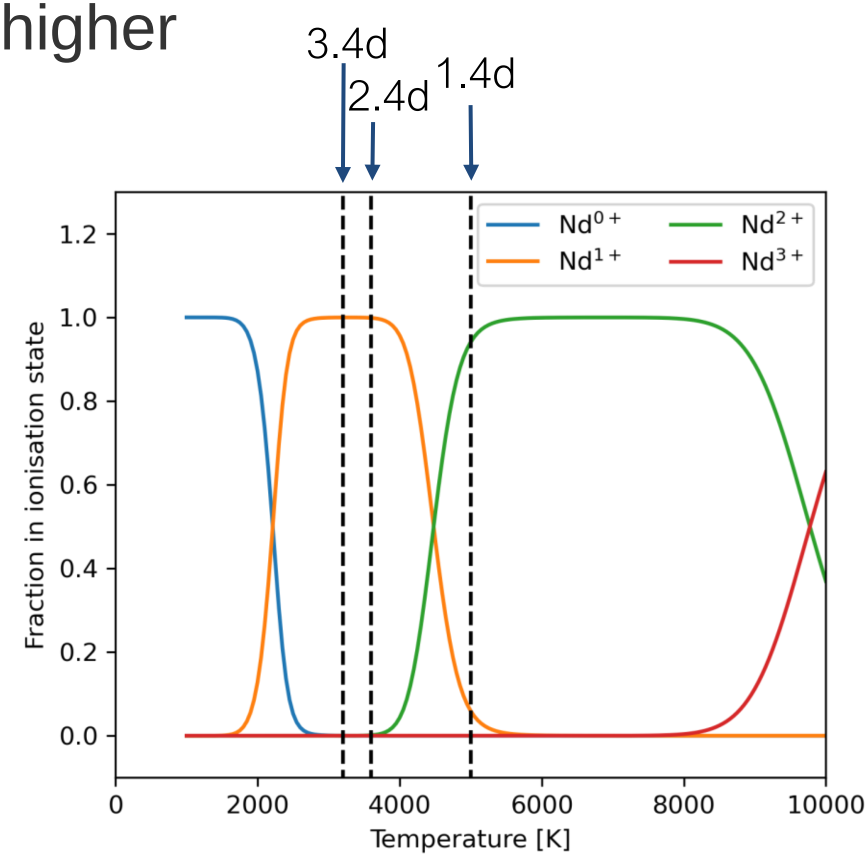

Level energies: Nd II

- Consider enough configurations to achieve convergence low lying states and level densities.
- Opacities after energy matching to known levels

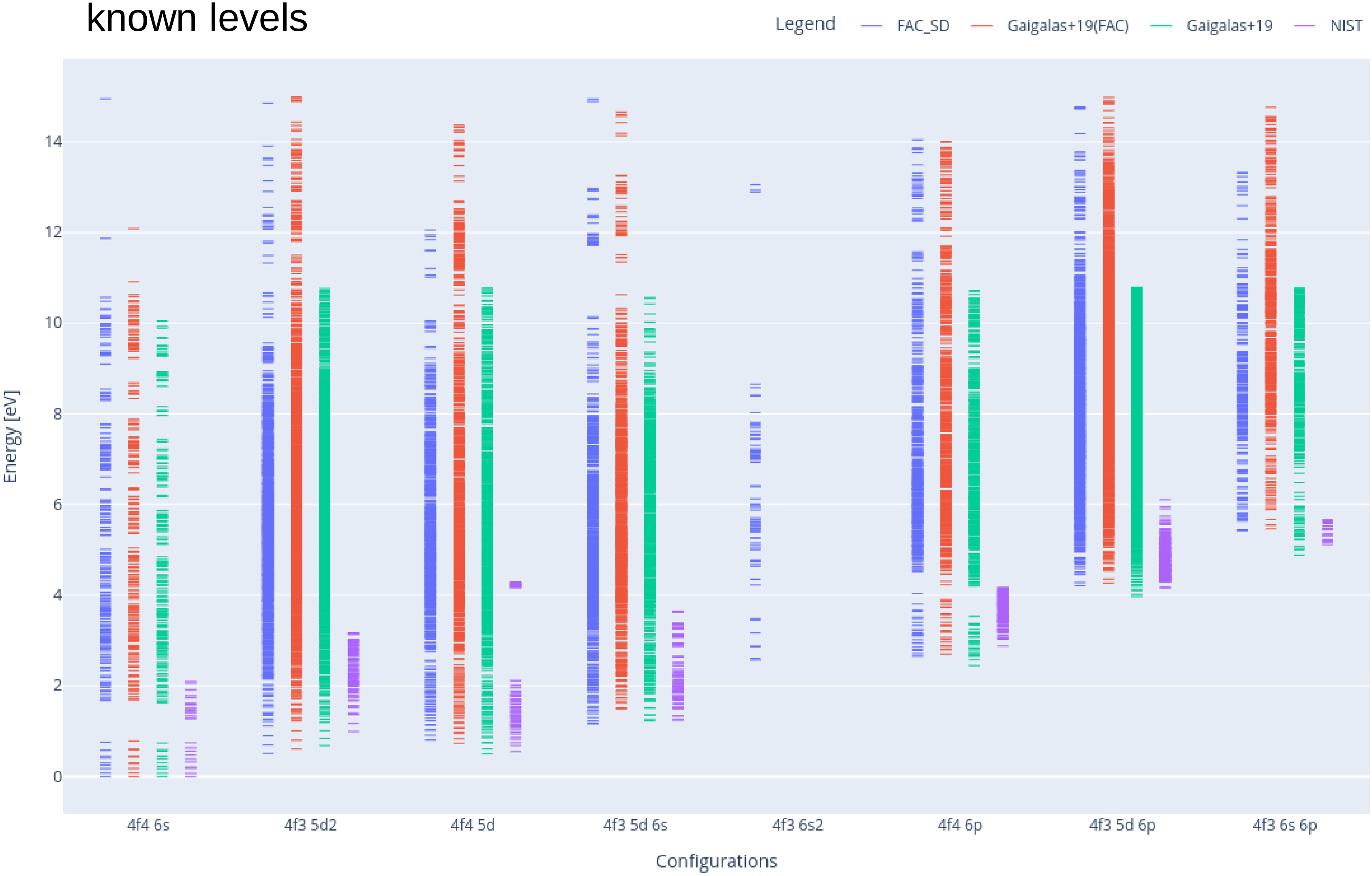

Level density: Nd II

- Large number configurations required to reproduce level density up to ionization energy

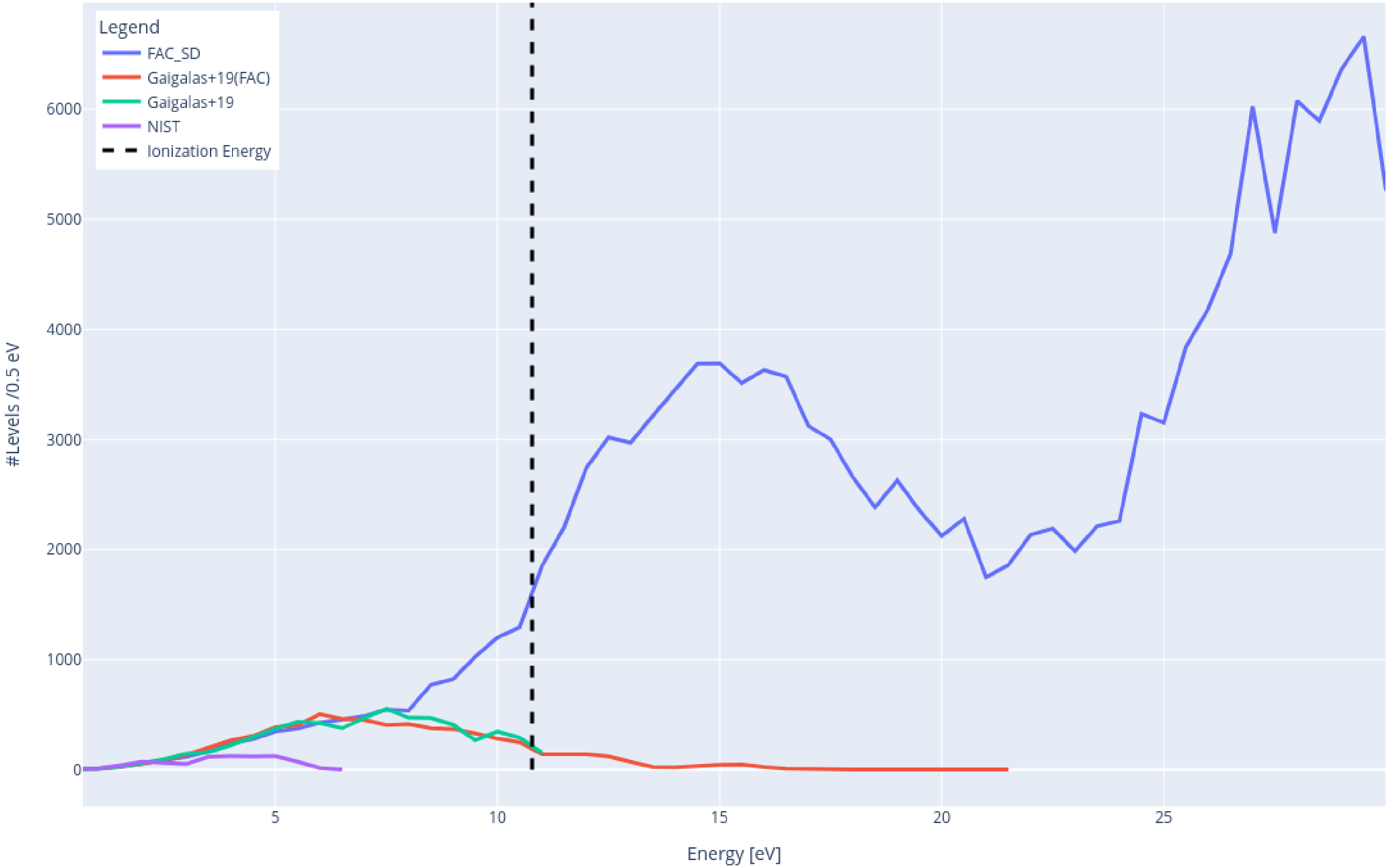

Expansion opacity: Nd II

- Good agreement with published results [Gaigalas et al, ApJS **240**, 29 (2019)]

- Small differences due to different atomic codes

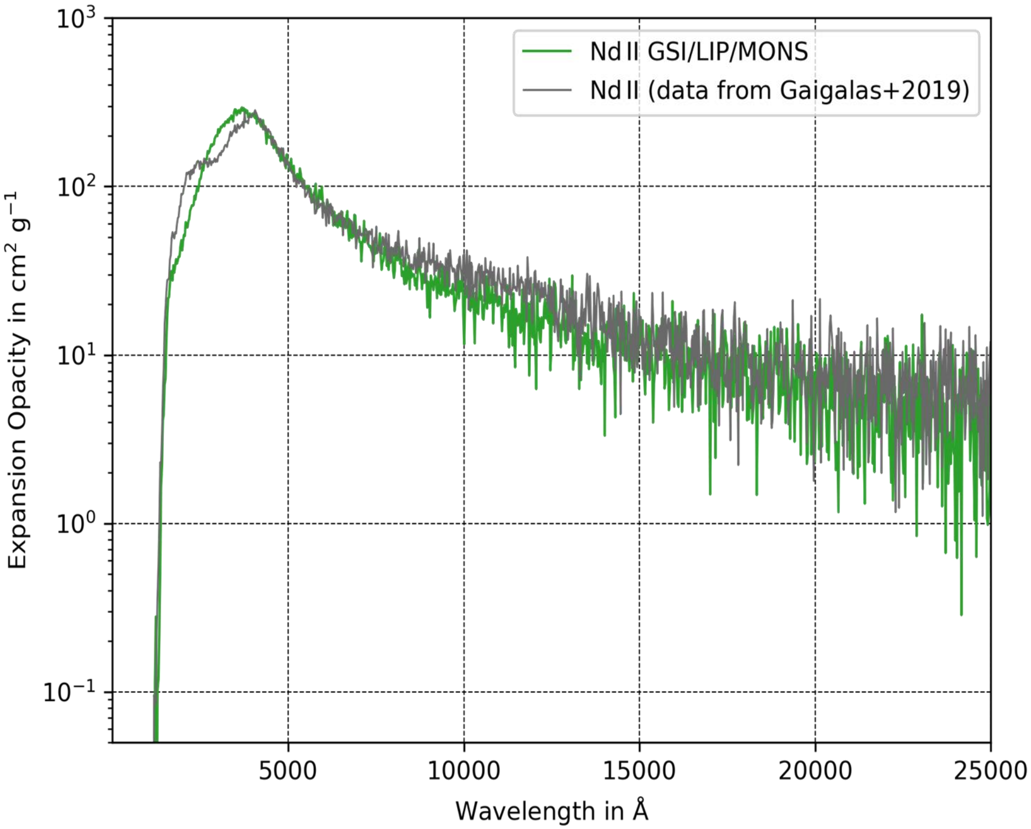

$$\rho = 10^{-13} \mathrm{g\,cm}^{-3} \quad T = 5000\ \mathrm{K}$$

Expansion opacity: Nd III

- Differences below 2000 Å
- Very limited measured data available
- Calibration to levels difficult

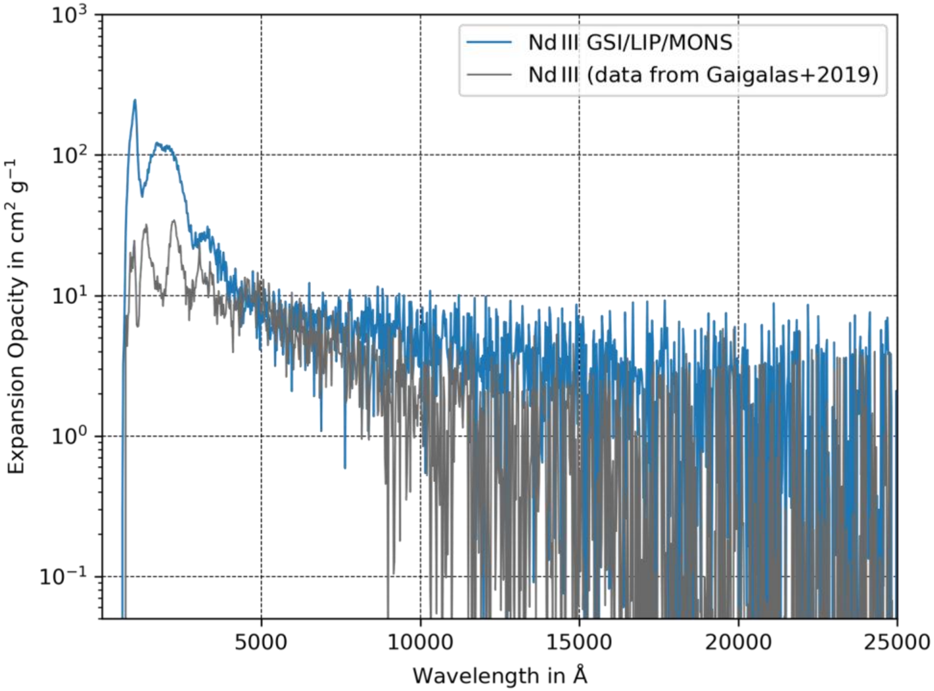

$$\rho = 10^{-13}\mathrm{g\ cm^{-3}} \quad T = 5000\ \mathrm{K}$$

Expansion opacity: Nd

Good agreement with Gaigalas+ 2019 for $T \lesssim 5000$ K

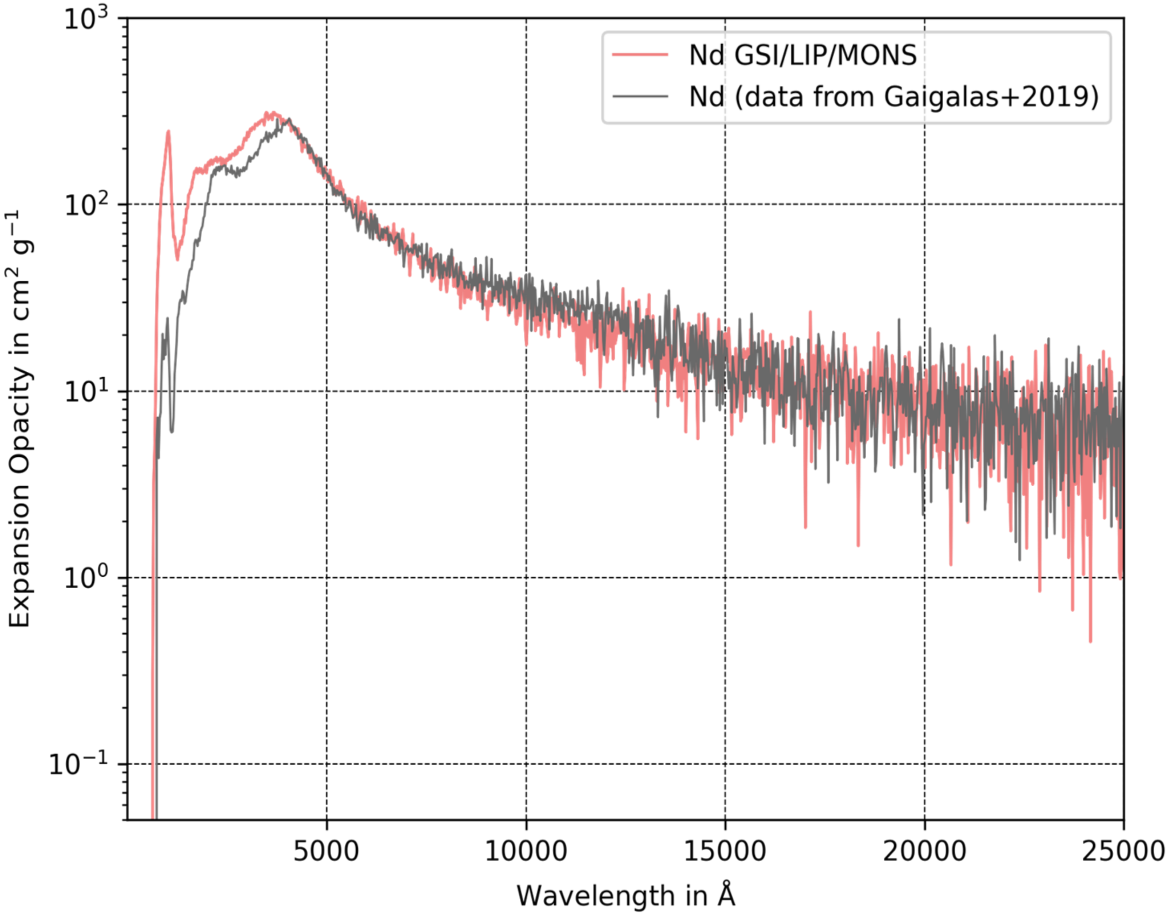

$$\rho = 10^{-13}\mathrm{g\,cm}^{-3} \quad T = 5000\ \mathrm{K}$$

Actinides vs Lanthanides

- How do the Actinides opacities compare to Lanthanides?
- Important to identify Actinides to determine what are the heavier elements produced.
- Actinides may be an important source of heating at late times (Zhu+ 2018, Wu+ 2019)

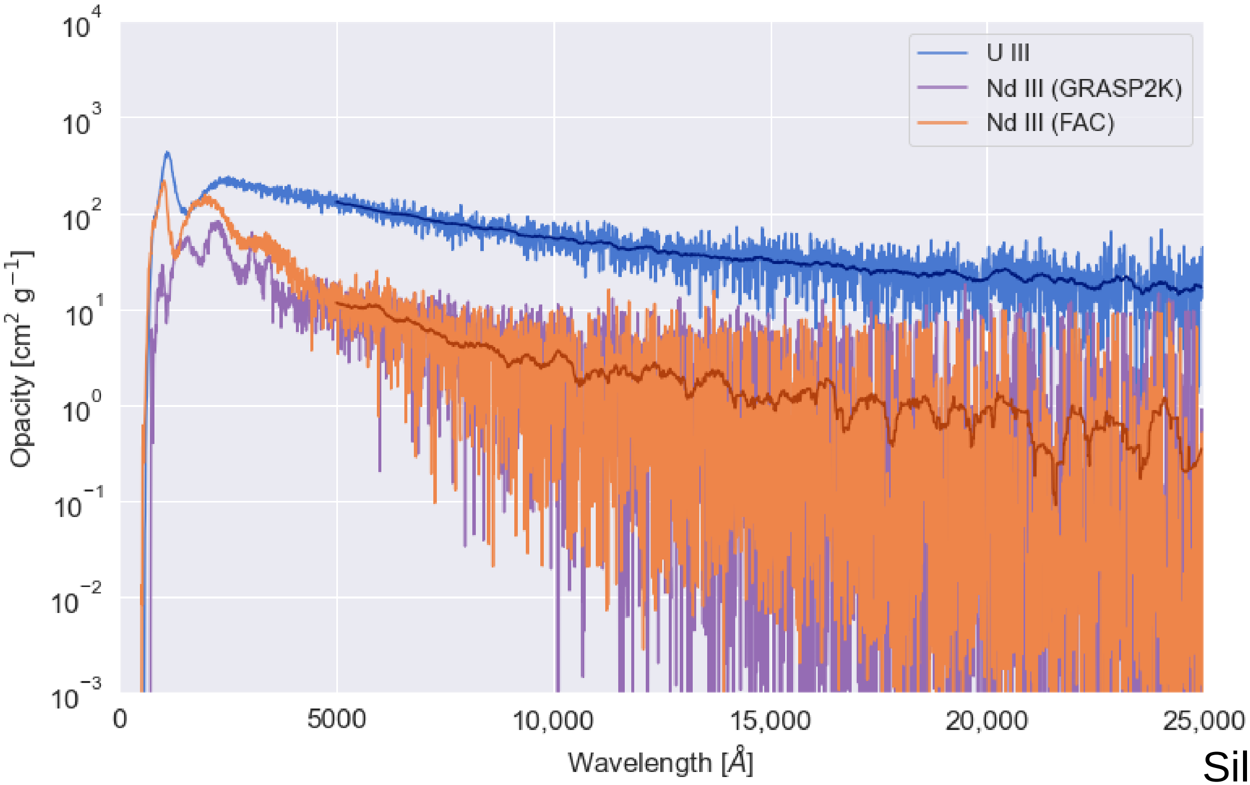

Larger opacities for U III than Nd III

No data available

Opens possibility of identifying features of actinides

Silva et al, Atoms 10, 18 (2022)

Expansion opacity: U III

- Benchmark against calculations using HFR code (U Mons). Confirms larger opacity of U III vs Nd III

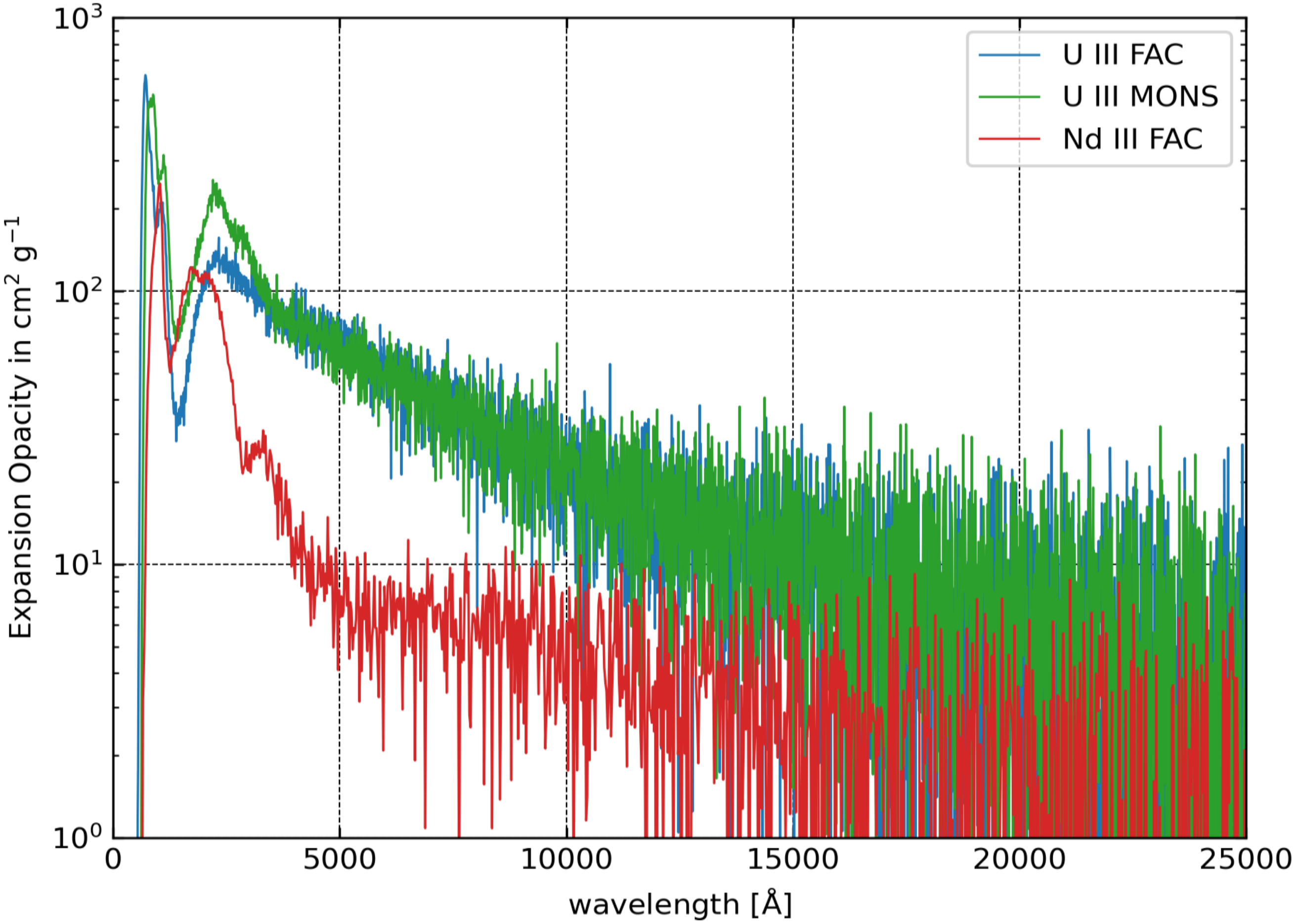

Extension to U II in progress

Modelling a Nd kilonova

A. Flörs

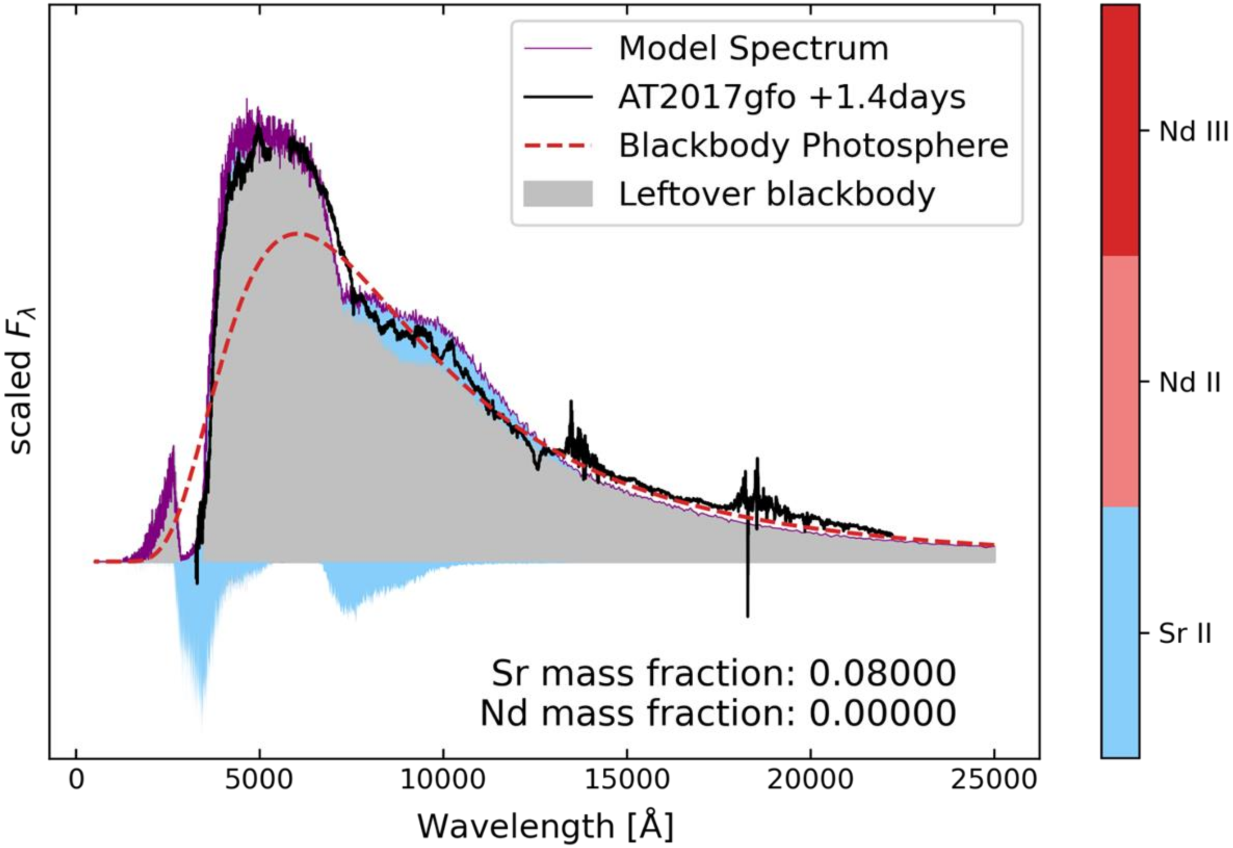

Exponential density profile

$$\rho(v,\, t_{\mathrm{exp}}) = \rho_0 \left(\frac{t_0}{t_{\mathrm{exp}}}\right)^3 \left(\frac{v}{v_0}\right)^{-\Gamma}$$

with power-law index $\Gamma = 3$

Increase the Nd mass fraction from 10^{-5} to 10^{-1}

Low abundance:
only line blanketing

High abundance:
line blanketing in addition to spectral features in the NIR

Modelling a Nd kilonova

A. Flörs

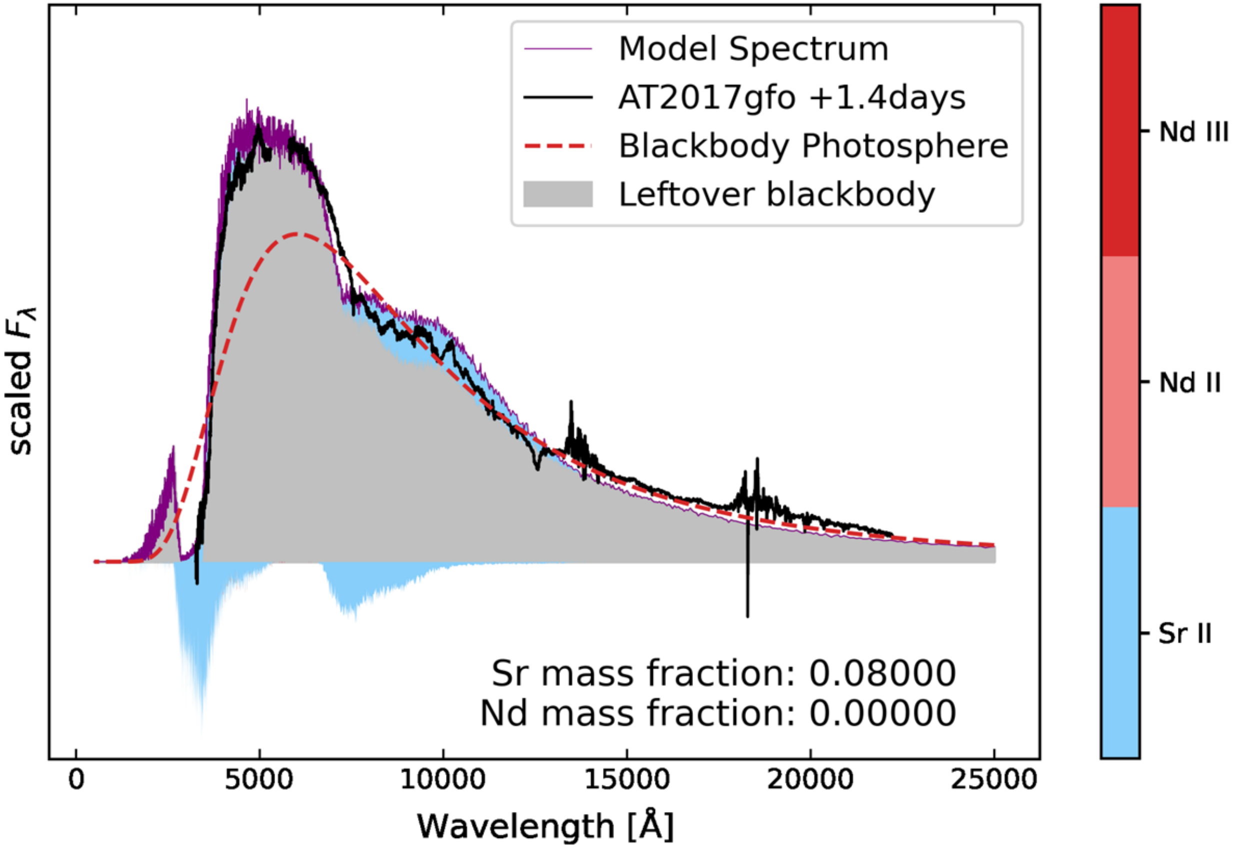

Exponential density profile

$$\rho(v, t_{\text{exp}}) = \rho_0 \left(\frac{t_0}{t_{\text{exp}}}\right)^3 \left(\frac{v}{v_0}\right)^{-\Gamma}$$

with power-law index $\Gamma = 3$

Increase the Nd mass fraction
from 10^{-5} to 10^{-1}

Low abundance:
only line blanketing

High abundance:
line blanketing in addition to spectral features in the NIR

ARTIS Developments

- Non-thermal particle deposition (Shingles+ 2020 and 2022, SN Ia):
  - continuous input of high-energy decay particles that do not thermalize efficiently, their energy distribution stays non-Maxwellian
  - non-thermal electron distribution by numerically solving the Spencer & Fano (1954) equation using the method of Kozma & Fransson (1992)
  - integrating over the energy distribution, we obtain rates for non-thermal ionization, excitation, and heating
- ARTIS developments for Kilonova
  - Kilonova: non-thermal effects expected as early as 3 days (Pognan+ 2022)
  - Non-thermal solver: non-LTE level populations, binned radiation field and detailed photoionisation rate estimators (Shingles+ 2020)
  - Decays included in a more generalize way
    - 2502 nuclides with alpha and beta-minus decay data from ENDF/B-VII.1 (Chadwick+ 2011 via Hotokezaka's data file)
    - Abundance calculation from Bateman equation describing decays (no capture reactions, no fission)
    - Gamma-ray decay spectra from NNDC and full transport
    - Particle emission using average kinetic energy per decay local but non-instantaneous deposition (assumed to be fully trapped)

L. Shingles

Light curve and spectra from mergers

- Dynamical ejecta from SPH simulations including neutrinos (ILEAS): simulation by V. Vijayan (1.35-1.35 $M_\odot$, SFHo EoS, 0.004 $M_\odot$ ejecta)

- Abundances determined from detailed network calculations

- 1D average (extension to 3D planned)

- ARTIS follows density (homologous) and abundance evolution (decays) while calculating radiative transfer

- Grey opacities based on Tanaka+ 2020 with Ye dependence. Future: line-by-line Sobolev treatment with detailed composition and NLTE level populations

L. Shingles

Radioactive heating: ARTIS vs network

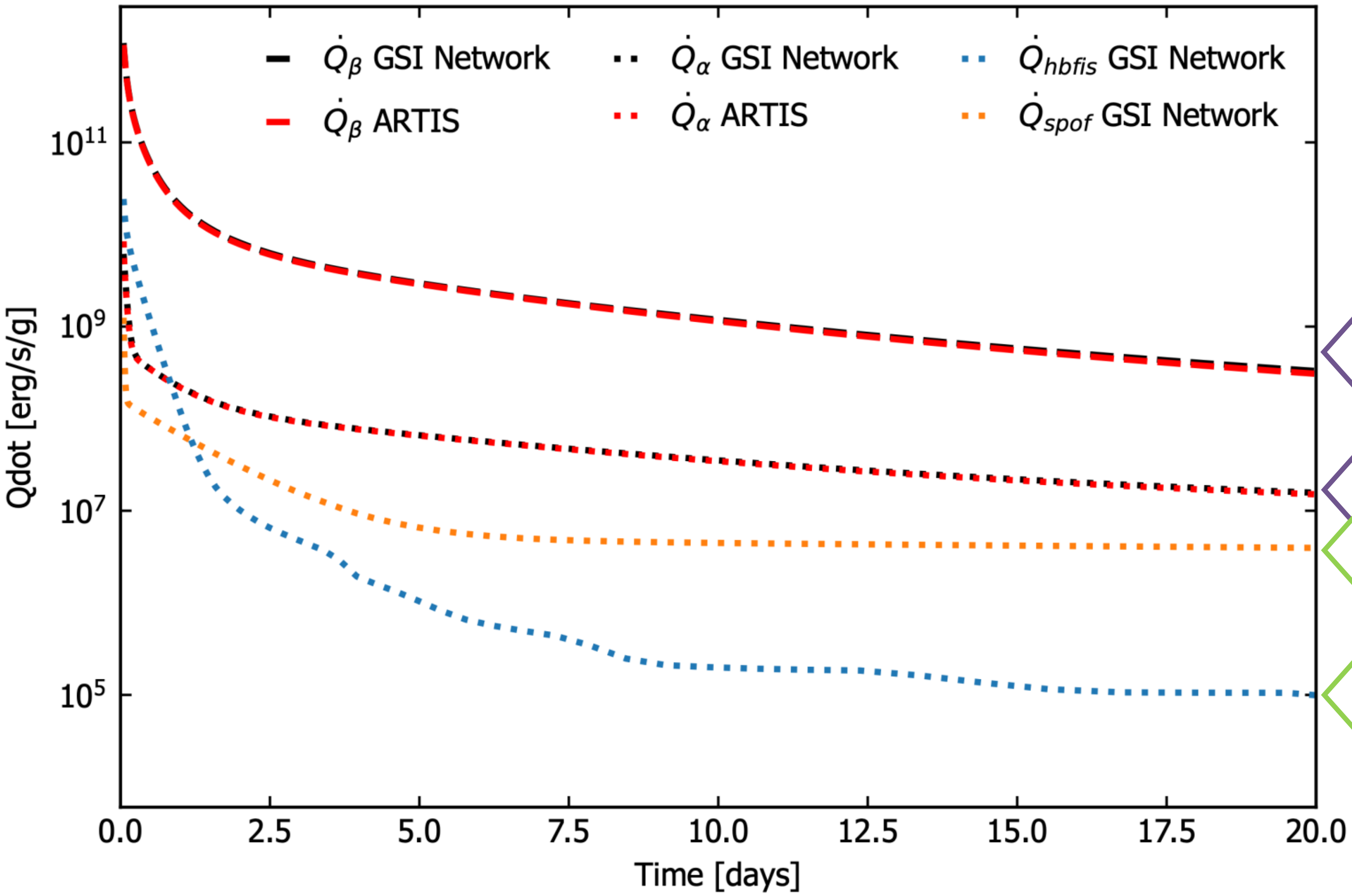

Good tracking of decay power

Fission not included, small contribution

Abundance evolution vs network

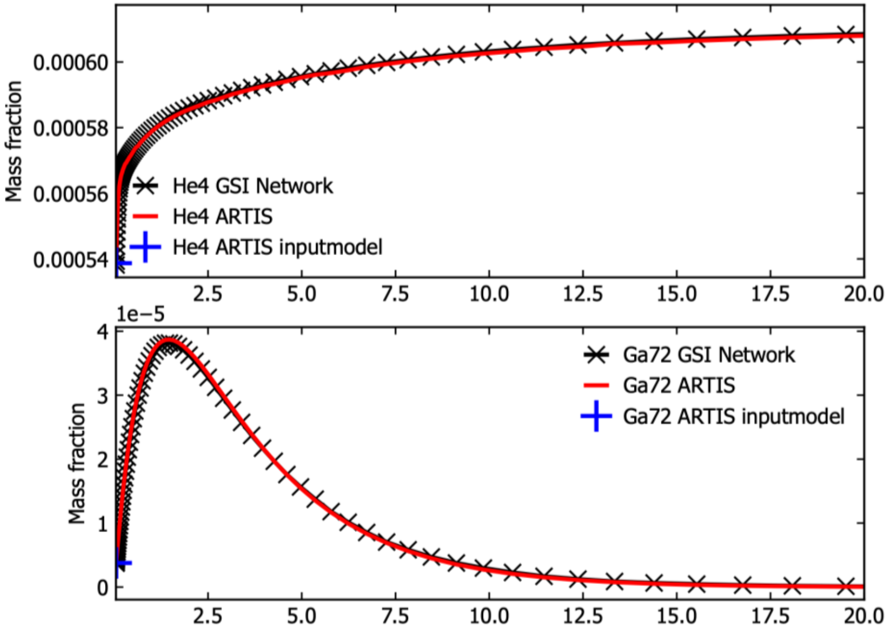

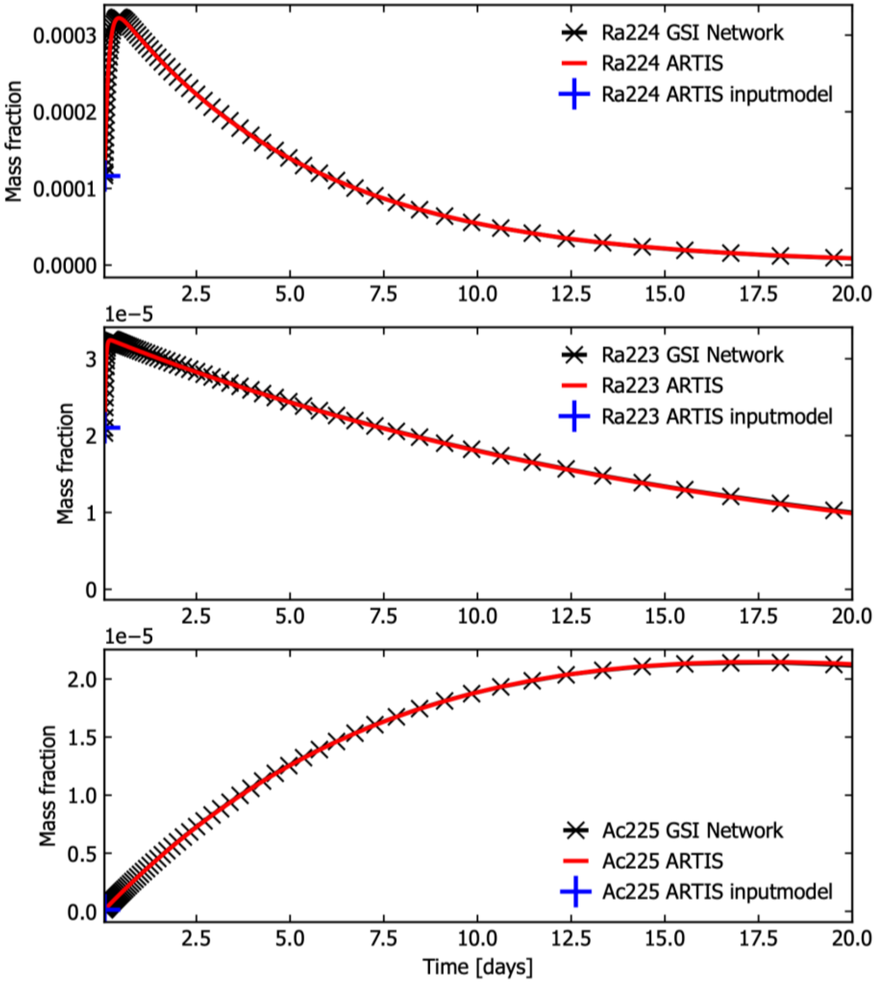

Thermalization results

Comparison with Barnes+ 2016 approximation

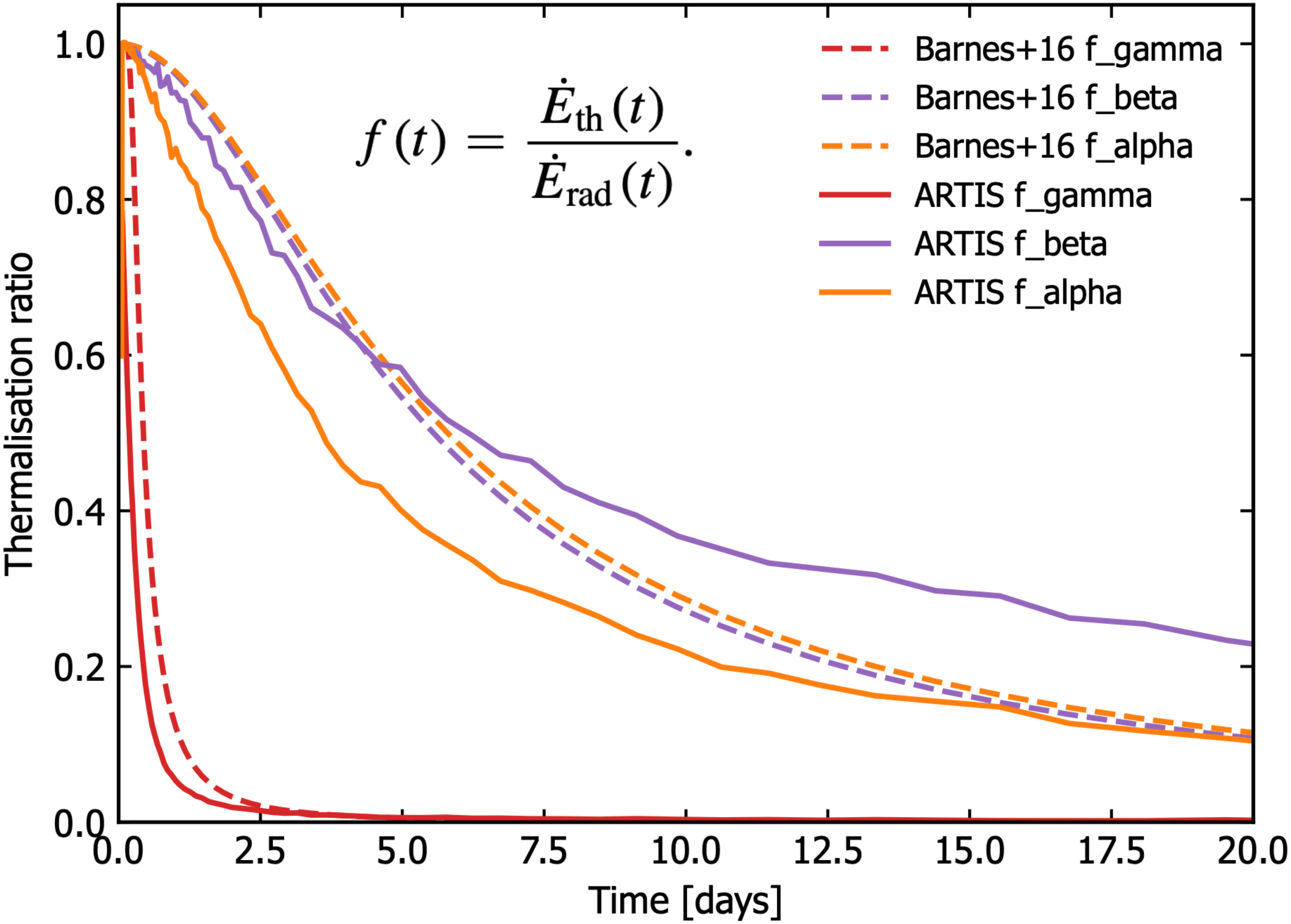

1D light curve

Ejected mass 0.004 $M_\odot$ is too low to explain AT2017gfo observations

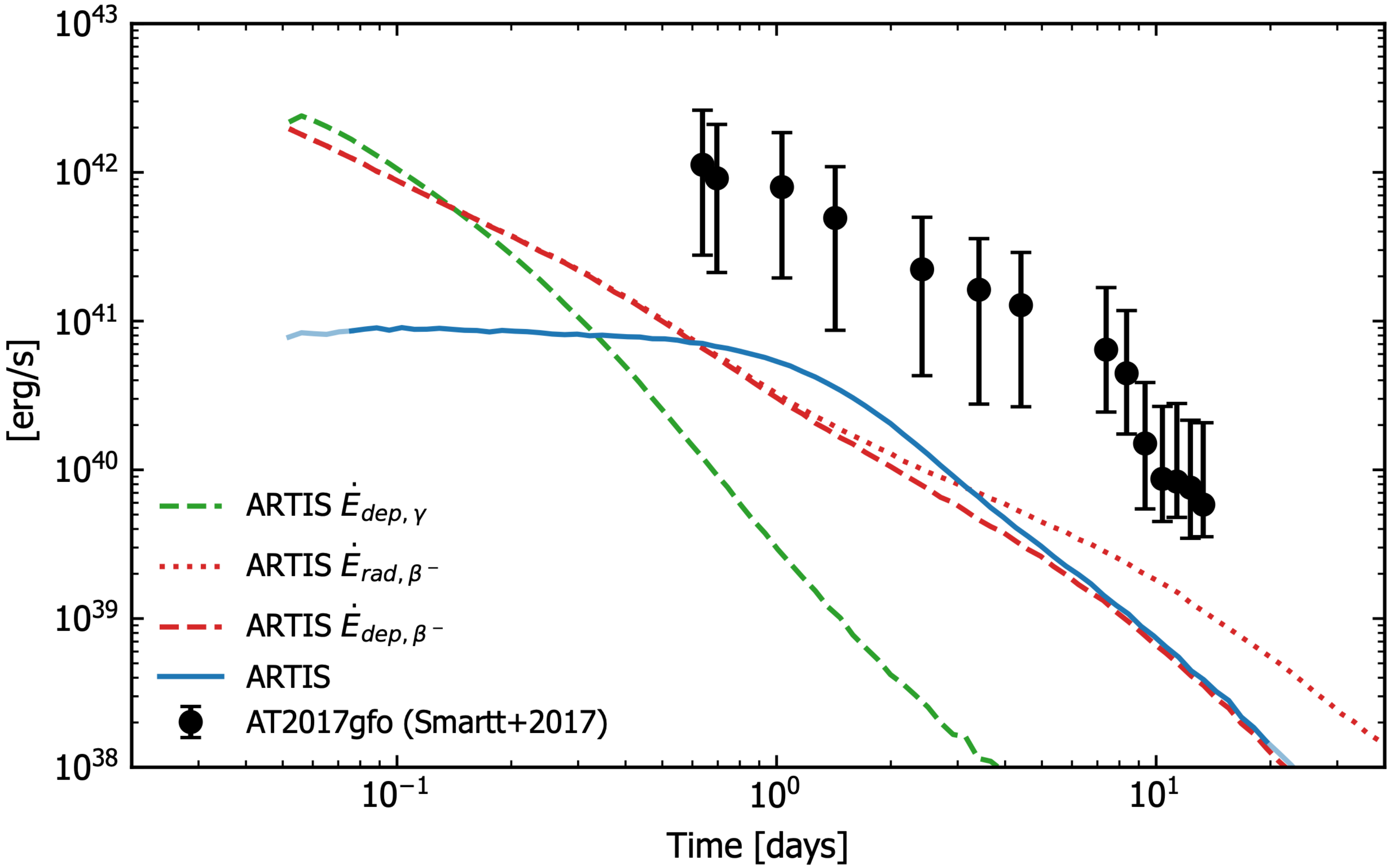

1D light curve

Ejected mass increased by a factor 10 to 0.04 $M_\odot$

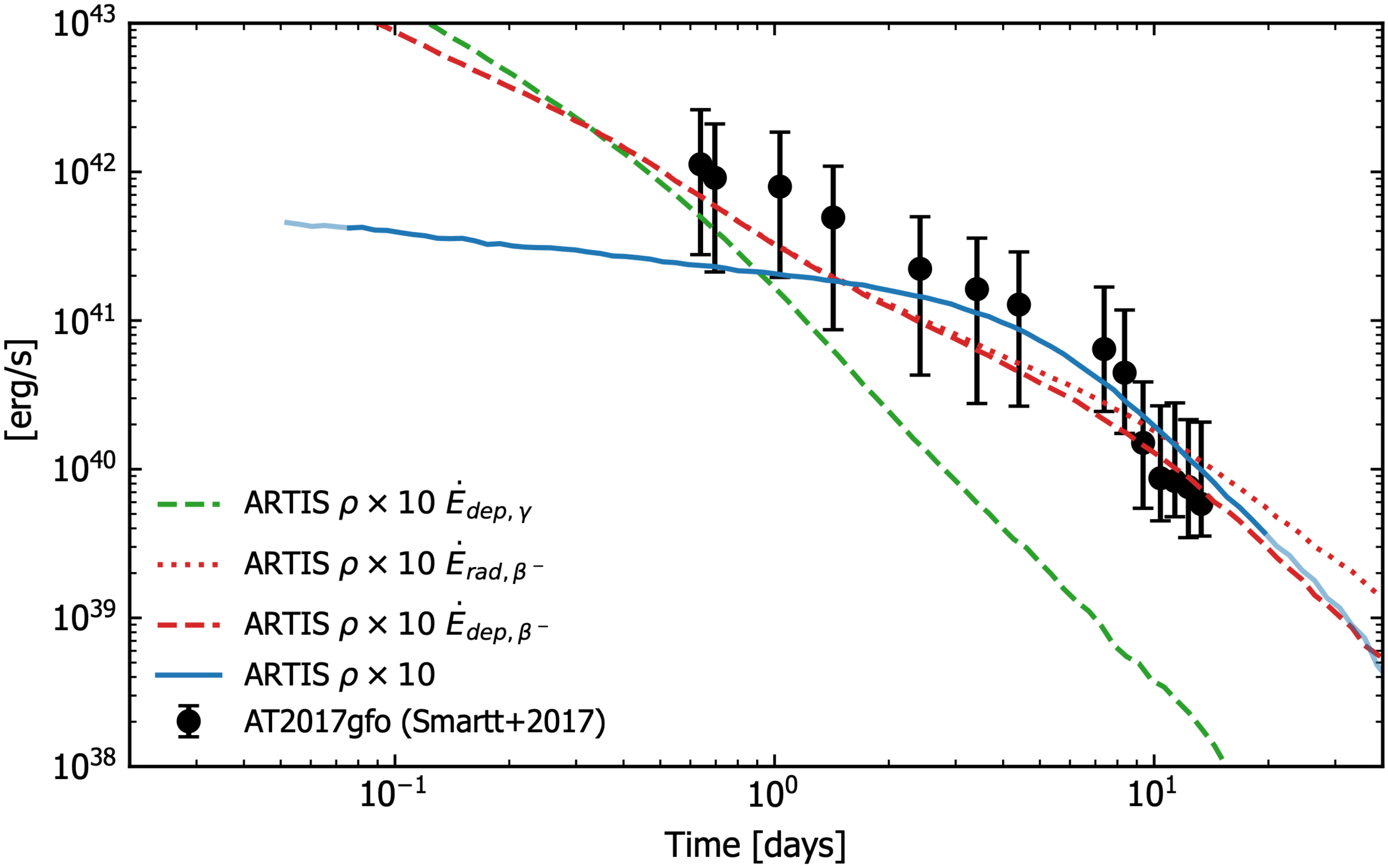

Late time break related to ejecta becoming transparent, nebular phase: Hotokezaka & Nakar, ApJ **891,** 152 (2020)

Summary

- Systematic calculations of bound-bound opacities in progress
  - Calibrated to data when available
  - Benchmarks of different atomic structure codes

- Implementation in radiative transfer codes TARDIS and ARTIS in progress

- Future: extension to Non-LTE (Nebular) phases.